J. Aerosol Sci. Vol. 11, pp. 397–402.

0021-8502/80/0701-0397 $02.00/0

DEPOSITION FROM CHARGED AEROSOL FLOWS THROUGH A PIPE BEND

C. K. DIU and C. P. YU

Department of Engineering Science, Aerospace Engineering and Nuclear Engineering, State University of New York at Buffalo, Buffalo, NY 14214, U.S.A.

(*Received* 18 *December* 1979)

Abstract – An analysis is presented on the deposition from a charged aerosol passing through a pipe bend. Collection efficiencies are found for different bend-to-pipe radius ratios. The results are compared with available experimental data.

INTRODUCTION

In a previous paper (Diu and Yu, 1980), we presented an analysis on the deposition from a charged aerosol flowing through a two-dimensional bend. In this paper, the same problem will be re-examined when the bend has a circular cross-section. Recent theoretical studies on inertial deposition in pipe bends were made by Cheng and Wang (1975) and Crane and Evans (1977). Cheng and Wang assumed an idealized rotational flow and found an analytical solution which shows that the collection efficiency in a 90° bend is almost independent of bend-to-pipe radius ratio. Crane and Evans considered a more realistic flow field including the secondary flow and calculated particle trajectories and collection efficiency numerically. Their results show that although particle trajectories depend strongly on the secondary flow, the collection efficiency is only affected by a small amount. The result of Cheng and Wang thus provides a good approximation for the collection efficiency.

In this study, the idealized rotational flow field used by Cheng and Wang will be adopted. The aerosol particles are assumed to be monodisperse and have a constant charge per particle. The particle concentration is assumed to be low so that the electrostatic force acting on each particle is only the image force due to its interaction with the wall.

BASIC EQUATIONS

The geometry of the problem is shown in Fig. 1. We consider a uniform aerosol entering a pipe bend of tube radius h and bend radius R with a bend angle θ_0. Employing the cylindrical

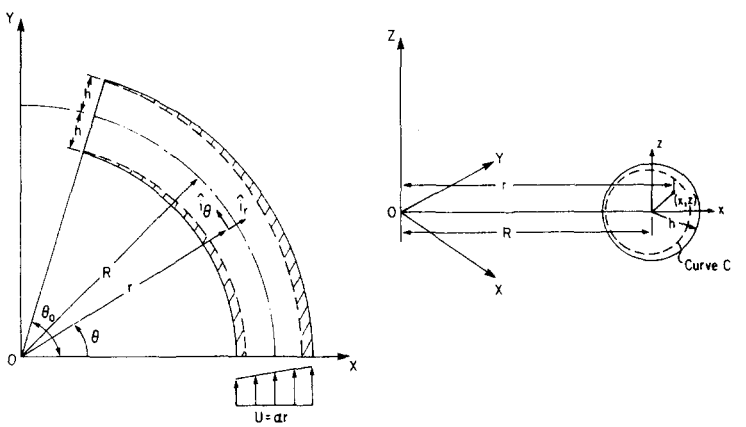

Fig. 1. Geometry of the pipe bend.

coordinates r, θ and z for the bend as shown, the air velocity then equals to $\alpha r\hat{i}_\theta$ where α is a constant, r is the distance from the axis of the bend to a point in the pipe and $\hat{i}_\theta$ is the unit vector in the θ direction. The equations of motion for a particle in the component form are

$$m(\ddot{r} - r\dot{\theta}^2) = -f\dot{r} + F_{er}, \tag{1}$$

$$m(r\ddot{\theta} + 2\dot{r}\dot{\theta}) = -fr(\dot{\theta} - \alpha), \tag{2}$$

and

$$m\ddot{z} = -f\dot{z} + F_{ez} \tag{3}$$

where the dot indicates the differentiation with respect to the time t, m is the particle mass, $f = 6\pi\mu a$ in which μ is the air viscosity and a is the particle radius, and F_{er} and F_{ez} are respectively the image force component in the r and z direction.

Similar to our previous paper, we assume that $\tau/T \ll 1$ and $h/R \ll 1$ where $\tau = m/f$ is the particle relaxation time and $T = \theta_0/\alpha$ is the residence time. Then, to the lowest approximation, equations (1)–(3) reduce to

$$-mr\dot{\theta}^2 = -f\dot{r} + F_{er}, \tag{4}$$

$$\dot{\theta} - \alpha = 0, \tag{5}$$

and

$$-f\dot{z} + F_{ez} = 0. \tag{6}$$

For the convenience of calculation, we introduce another coordinate system xyz as shown in Fig. 1 such that its origin coincides with the center of the pipe and the x-axis is along the r direction. Then $r = R + x$ and $x^2 + z^2 = h^2$ describes the wall of the tube. The image force on a particle in the conducting bend is approximated by the expression for a straight tube. This gives (Yu, 1977)

$$F_{er} = \frac{Q^2}{16\pi\varepsilon_0 h^2} \frac{\sqrt{x^2 + z^2}}{(h - \sqrt{x^2 + z^2})^2} x, \tag{7}$$

and

$$F_{ez} = \frac{Q^2}{16\pi\varepsilon_0 h^2} \frac{\sqrt{x^2 + z^2}}{(h - \sqrt{x^2 + z^2})^2} z \tag{8}$$

in which Q is the particle charge.

We eliminate $\dot{\theta}$ from equation (4) with the use of equation (5) and substitute equations (7) and (8) into the resulting equation and also in equation (6). This gives

$$\frac{dx^*}{dt^*} = E \frac{\sqrt{x^{*2} + z^{*2}}}{(1 - \sqrt{x^{*2} + z^{*2}})^2} x^* + I(S + x^*), \tag{9}$$

and

$$\frac{dz^*}{dt^*} = E \frac{\sqrt{x^{*2} + z^{*2}}}{(1 - \sqrt{x^{*2} + z^{*2}})^2} z^* \tag{10}$$

where * indicates non-dimensional quantities of x, z and t such that $x^* = x/h$, $z^* = z/h$ and $t^* = \alpha t/\theta_0$ and I, E and S are non-dimensional parameters, defined by

$$I = Stk\,\theta_0/S, \tag{11}$$

$$E = \frac{Q^2\theta_0}{16\pi\varepsilon_0 h^3 f\alpha} \tag{12}$$

and

$$S = R/h. \tag{13}$$

In equation (11), $Stk = \tau\alpha R/h$ is the Stokes number.

COLLECTION EFFICIENCY

Following the procedure we developed previously (Thiagarajan and Yu, 1979), equations (9) and (10) are solved numerically to obtain the limiting trajectories. One can identify a closed curve C symmetric to the x-axis at the entrance of the bend, (see Fig. 1), such that the particle entering through this curve will deposit on the wall at $t^* = 1$. The collection efficiency is then

$$\eta = 1 - \frac{\iint_A \alpha(S + x^*)\mathrm{d}x^*\,\mathrm{d}z^*}{\iint_{x^{*2}+z^{*2}=1} \alpha(S + x^*)\mathrm{d}x^*\,\mathrm{d}z^*} \tag{14}$$

where A is the area bounded by the curve C.

When $E = 0$, i.e. only inertial deposition is considered, we have

$$\frac{\mathrm{d}x^*}{\mathrm{d}t^*} = I(S + x^*). \tag{15}$$

This gives

$$\int_{x_c^*}^{x_b^*} \frac{\mathrm{d}x^*}{I(S + x^*)} = \int_0^1 \mathrm{d}t^* = 1 \tag{16}$$

or

$$\frac{S + x_b^*}{S + x_c^*} = e^I \tag{17}$$

where x_b^* and x_c^* correspond, respectively, to the values of x^* on the wall and the curve C at a constant z^* (Fig. 2). The collection efficiency η in this case is

$$\eta = 1 - \frac{\int_0^{z_{cm}^*}\int_{x_b^*}^{x_c^*} \alpha(S + x^*)\mathrm{d}x^*\,\mathrm{d}z^*}{\int_0^1 \int_{x_b^{*'}}^{x_b^*} \alpha(S + x^*)\mathrm{d}x^*\,\mathrm{d}z^*} \tag{18}$$

where $x_b^* = \sqrt{1 - z_b^{*2}}$, $x_b^{*'} = -\sqrt{1 - z_b^{*2}} = -x_b^*$ and z_{cm}^* is the maximum value of z_c^*, given by

$$z_{cm}^* = \left[1 - S^2\left(1 - \frac{2}{e^I + 1}\right)^2\right]^{1/2}. \tag{19}$$

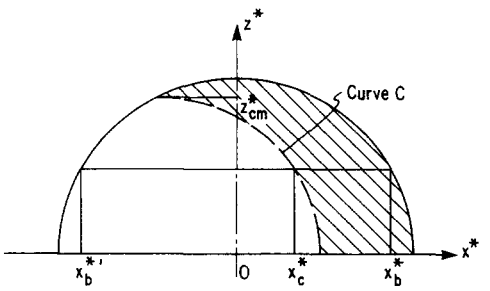

Fig. 2. Critical location curve C for inertial deposition in a 90° bend.

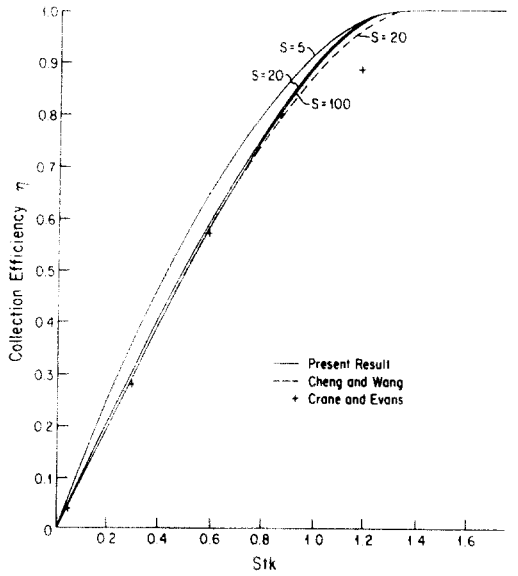

Fig. 3. Collection efficiency vs Stokes number for pure inertial deposition ($E = 0$) in a 90° bend.

We solve x_c^* from equation (17) and substitute the result into equation (18), after carrying out the integral, we finally obtain

$$\eta = 1 - \frac{1 + e^{-2I}}{\pi}(\sin^{-1} z_{cm}^* + z_{cm}^*\sqrt{1 - z_{cm}^{*2}}) + \frac{1}{\pi S}(1 - e^{-2I})z_{cm}^*\left(S^2 + 1 - \frac{z_{cm}^{*2}}{3}\right). \quad (20)$$

RESULTS AND DISCUSSION

Equation (20) is a simpler expression for η than that obtained previously by Cheng and Wang. The reason for the difference between the two results is that we have dropped the terms $(m/f)\ddot{r}$ and $(m/f)\ddot{z}$ in equations (1) and (3) since they are small compared with the terms $\dot{r}$ and $\dot{z}$ in those equations. Figure 3 shows the collection efficiency η of a 90° bend calculated from equation (20) vs the Stokes number Stk for several values of S. It is seen that η is almost independent of S as noted previously. The results of Cheng and Wang and Crane and Evans

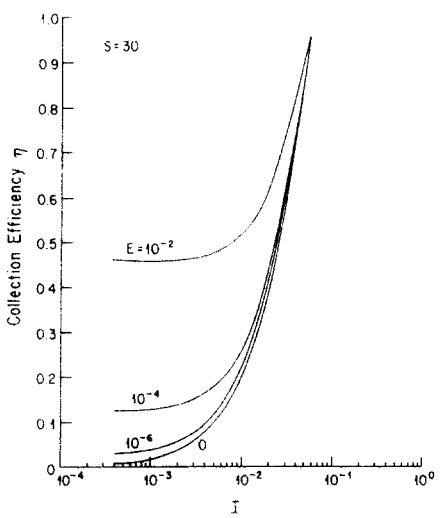

Fig. 4. Collection efficiency of a 90° bent tube vs I for $S = 30$ and several values of E

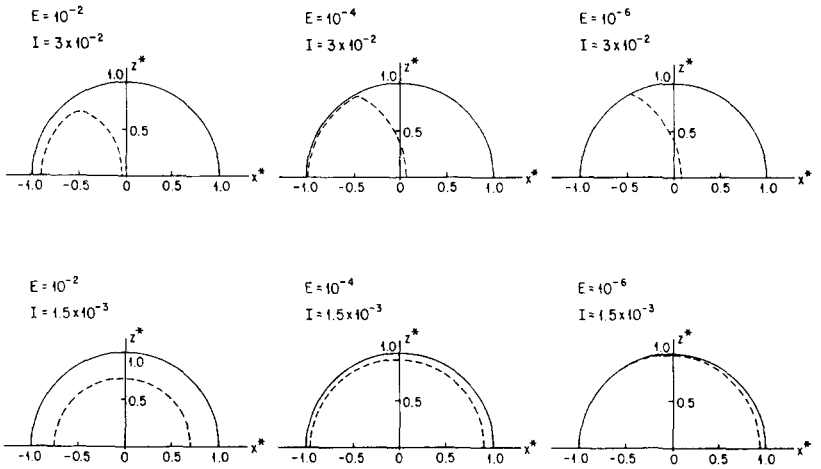

Fig. 5. Changes in curve C at the bend entrance as E decreases for different values of I in a 90° bend.

for $S = 20$ are also plotted in Fig. 3 for comparison. They agree very well with the present result.

For charged aerosols, the collection efficiency will depend upon the parameters I, S as well as E. Figure 4 shows the effect of E on η for $S = 30$. Significant increase of η due to the increase of E is observed. This increase is attributed to the additional electrostatic image force acting on the particle. The changes in location for the curve C at the bend entrance as E increases are shown in Fig. 5.

Chan *et al.* (1978) have studied the charge effect on the deposition of particles in a lung cast. They found a significant increase in deposition in the trachea for $Stk < 0.02$ when the particle carries 360–1100 negative charge units. A comparison of these experimental data with the present theoretical results is shown in Fig. 6. The theoretical calculations were made for 1 μm dia. particles flowing through a 90° bend of 1 cm tube diameter. Results for both charged and uncharged particles are presented. Agreement between theory and experiment appears reasonably good.

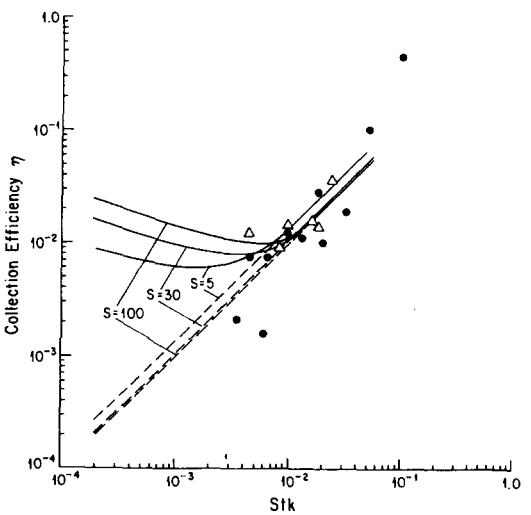

Fig. 6. Collection efficiency of a 90° bend vs Stokes number for several values of S when an aerosol of 1 μm aerodynamic diameter is flowing through a bend of 1 cm dia. The dotted lines are for $Q = 0$ and the solid lines are for $Q = 300$ electronic charges. The experimental values of deposition efficiency in the trachea with uncharged particle, ●, and with negatively charged particles of 360–1100 charges/particle, △, are presented for comparison.

Acknowledgement – This work was supported jointly by the National Institute of Environmental Health Sciences and the Environmental Protection Agency under Grant No. ES 1239 and by the National Institute for Occupational Safety and Health under Grant No. OH-923.

REFERENCES

Chan, T. L., Lippmann, M., Cohen, V. R. and Schlesinger, R. B. (1978) *J. Aerosol Sci.* **9,** 463.
Cheng, Y. S. and Wang, C. S. (1975) *J. Aerosol Sci.* **6,** 139.
Crane, R. I. and Evans, R. I. (1977) *J. Aerosol Sci.* **8,** 161.
Diu, C. K. and Yu, C. P. (1980) *J. Aerosol Sci.* **11,** 383.
Thiagarajan, V. and Yu, C. P. (1979) *J. Aerosol Sci.* **10,** 405.
Yu, C. P. (1977) *J. Aerosol Sci.* **8,** 237.